Monthly Notices
of the
ROYAL ASTRONOMICAL SOCIETY

MNRAS **453,** L31–L35 (2015) doi:10.1093/mnrasl/slv094

Gas-phase formation of the prebiotic molecule formamide: insights from new quantum computations

V. Barone,[1⋆] C. Latouche,[1] D. Skouteris,[1⋆] F. Vazart,[1] N. Balucani,[2,3,4] C. Ceccarelli[3,4⋆] and B. Lefloch[3,4]

[1] *Scuola Normale Superiore, Piazza dei Cavalieri 7, I-56126 Pisa, Italy*
[2] *Dipartimento di Chimica, Biologia e Biotecnologie, Via Elce di Sotto 8, I-06123 Perugia, Italy*
[3] *Univ. Grenoble Alpes, IPAG, F-38000 Grenoble, France*
[4] *CNRS, IPAG, F-38000 Grenoble, France*

Accepted 2015 July 13. Received 2015 July 2; in original form 2015 July 2

ABSTRACT

New insights into the formation of interstellar formamide, a species of great relevance in prebiotic chemistry, are provided by electronic structure and kinetic calculations for the reaction $NH_2 + H_2CO \rightarrow NH_2CHO + H$. Contrarily to what previously suggested, this reaction is essentially barrierless and can, therefore, occur under the low temperature conditions of intestellar objects thus providing a facile formation route of formamide. The rate coefficient parameters for the reaction channel leading to $NH_2CHO + H$ have been calculated to be $A = 2.6 \times 10^{-12}$ cm^3 s^{-1}, $\beta = -2.1$ and $\gamma = 26.9$ K in the range of temperatures 10–300 K. Including these new kinetic data in a refined astrochemical model, we show that the proposed mechanism can well reproduce the abundances of formamide observed in two very different interstellar objects: the cold envelope of the Sun-like protostar IRAS16293−2422 and the molecular shock L1157-B2. Therefore, the major conclusion of this Letter is that there is no need to invoke grain-surface chemistry to explain the presence of formamide provided that its precursors, NH_2 and H_2CO, are available in the gas phase.

Key words: ISM: abundances – ISM: molecules.

1 INTRODUCTION

Interstellar molecules including a peptide bond –NH–C(=O)–, such as formamide (NH_2CHO) and acetamide (NH_2COCH_3), are particularly interesting for their potential role in prebiotic chemistry (Saladino et al. 2012). Formamide was detected for the first time in space towards Sgr B2 by Rubin et al. (1971) and later in Orion KL (Turner 1989). Since then, it has been observed in several massive hot cores (Bisschop et al. 2007; Adande, Woolf & Ziurys 2011), low-mass hot corinos (Lopez-Sepulcre et al. 2015), the cold envelope and hot corino of IRAS16293-2422 (Kahane et al. 2013), and the outflow shock regions L1157-B1 and B2 (Yamaguchi et al. 2012; Mendoza et al. 2014). Formamide was also detected in the Hale–Bopp comet (Bockelee-Morvan et al. 2000) and, more recently, in comets C/2012 F6 and C/2013 R1 (Biver et al. 2014). Therefore, formamide is present in a large variety of star-forming environments, as well as in Solar system comets, thus supporting the hypothesis that molecules with a strong prebiotic potential could have been delivered to Earth by comets after being synthesized in pre-stellar environments (e.g. Caselli & Ceccarelli 2012).

In a very recent study by Lopez-Sepulcre et al. (2015), formamide has been searched for in ten low- and intermediate-mass pre-stellar and protostellar objects as a part of the IRAM Large Programme ASAI (Astrochemical Surveys At IRAM), which makes use of unbiased broad-band spectral surveys at millimetre wavelengths. While the related species HNCO (isocyanic acid) has been detected in all objects, formamide has not been identified in five of them, which are the coldest and devoid of hot corinos. According to those results, Lopez-Sepulcre et al. (2015) suggested that HNCO is formed in the gas phase during the cold stages of star formation, while NH_2CHO is formed from the hydrogenation of HNCO on the ice mantles of dust grains and remains frozen until the temperature rises enough to cause the icy grain mantles to sublimate. Nevertheless, very recent experimental work on the hydrogenation of the frozen HNCO seems to dispute the suggestion that HNCO is the parent species of NH_2CHO on ice (Noble et al. 2015). Other heterogeneous processes on the icy surface of interstellar grains have also been considered (Garrod, Weaver & Herbst 2008; Jones, Bennett & Kaiser 2011; Walsh et al. 2014).

The formation routes of NH_2CHO in the gas phase have been only partially investigated. Quan & Herbst (2007) suggested that the radiative association reaction between formaldehyde and protonated ammonia followed by dissociative electron recombination could be a source of formamide. However, the model of Quan & Herbst could only produce an abundance of formamide of $\sim 10^{-15}$

⋆ E-mail: vincenzo.barone@sns.it (VB); dimitrios.skouteris@sns.it (DS); Cecilia.Ceccarelli@obs.ujf-grenoble.fr (CC)

(with respect to H_2), significantly lower than the value found by Hollis et al. (2006) in Sgr B2. Instead of radiative association, Halfen, Ilyushin & Ziurys (2011) suggested that the ion–molecule reaction between formaldehyde and protonated ammonia could lead to protonated formamide, which, in turn, forms formamide by dissociative recombination according to $NH_3CHO^+ + e^- \rightarrow NH_2CHO + H$. A recent theoretical study of the reaction $NH_4^+ + H_2CO$ confuted this suggestion (Redondo, Barrientos & Largo 2014b) because it was verified that all the channels of the potential energy surface (PES) leading to protonated formamide exhibit high-energy barriers. The feasibility of other gas-phase ion–molecule reactions that could produce precursors of formamide has been recently explored by Redondo, Barrientos & Largo (2014a) who considered the ion–molecule reactions between NH_3OH^+ and NH_2OH^+ with H_2CO and HCOOH. Also in these cases, the presence of high-energy barriers along the reaction pathways has been exhibited.

As for neutral–neutral reactions, the $NH_2 + H_2CO \rightarrow NH_2CHO + H$ seems to be a viable route and, indeed, this reaction has been initially considered in the OSU data base (Garrod et al. 2008; http://faculty.virginia.edu/ericherb) with an estimated rate coefficient in the gas kinetics range (10^{-10} cm^3 s^{-1}), with the assumption that it is a barrier-less reaction. Later on, however, Garrod (2013) disregarded such an assumption with the following reasons. According to the theoretical study by Li & Lu (2002), the more exothermic product channel leading to $NH_3 + HCO$ is characterized by an entrance barrier of 5.89 kcal mol^{-1} ($\sim$ 3000 K) with an estimated rate coefficient of 5.25×10^{-17} cm^3 s^{-1}. Li & Lu (2002) investigated only the channel leading to $NH_3 + HCO$. None the less, Garrod (2013), by drawing an analogy with the reaction $OH + H_2CO$ where the channel leading to $HCOOH + H$ has a branching ratio of $\sim$2 per cent compared to the dominant $H_2O + HCO$ channel, concluded that the role of the $NH_2 + H_2CO \rightarrow NH_2CHO + H$ must be irrelevant. The reaction was therefore excluded from the gas-phase network and rather considered a possible formation route of formamide when in ice-assisted chemistry (Garrod 2013; Garrod et al. 2008).

In this work, we present state of the art quantum mechanical characterizations of the characteristic stationary points (minima and first-order saddle points, also referred to as transition states) on the PES governing the $NH_2 + H_2CO$ reaction channels (Sections 2 and 3). At variance from previous suggestions by Garrod (2013) and Garrod et al. (2008), the reaction pathway proceeding with the addition of the nitrogen atom of the NH_2 group to the carbon atom of formaldehyde has been found to be essentially barrierless. Actually, the entrance channel is characterized by a minimum corresponding to a van der Waals complex followed by a first-order saddle point, but both stationary points lie below the asymptotic reactants energy according to CBS-QB3 calculations. We have chosen to treat the van der Waals region adiabatically rather than assume that energy randomization takes place at the minimum, as such a process is not expected to be efficient. For this reason, we have also employed capture theory as well as Rice–Ramsperger–Kassel–Marcus (RRKM) calculations to derive the reaction rate coefficient as a function of the temperature in the range between 10 and 300 K, that is, the range of relevance for the interstellar objects of interest. The approach is the same as recently used by us to investigate a bimolecular formation route of cyanomethanimine, another complex organic molecule with a prebiotic potential (Vazart et al. 2015). The derived rate coefficient has also been tested in astrochemical models and compared with the formamide abundance measured in star formation regions (Section 4). A final section (Section 5) discusses the implications of the computations presented here and the future perspectives.

2 COMPUTATIONAL DETAILS

2.1 Electronic calculations

All calculations have been performed with a development version of the Gaussian suite of programs (Frisch et al. 2013). Most of the computations were performed with the double-hybrid B2PLYP functional (Grimme 2006) in conjunction with the m-aug-cc-pVTZ basis set (Dunning 1989; Papajak et al. 2009) where *d* functions on hydrogens have been removed. Semi-empirical dispersion contributions were also included by means of the D3BJ model of Grimme (Goerigk & Grimme 2011; Grimme, Ehrlich & Goerigk 2011). Full geometry optimizations have been performed for all molecules checking the nature of the obtained structures (minima or first-order saddle points) by diagonalizing their Hessians. More accurate electronic energies were obtained by the complete basis set (CBS-QB3) method, which employs a coupled cluster ansatz including single and double excitations together with a perturbative estimation of triple excitations (CCSD(T)) in conjunction with complete basis set extrapolation (Ochterski, Petersson & Montgomery 1996; Montgomery et al. 2000).

2.2 Kinetic calculations

We have performed kinetic calculations using an in house code described in previous papers (Leonori et al. 2009, 2013; Vazart et al. 2015). The initial bimolecular rate constant leading from the reactants to the intermediate is evaluated using capture theory calculations, after fitting the energy values for the approaching reactants to a $1/R^6$ functional form and assuming that each successful capture leads to the intermediate. As far as dissociation back to reactants is concerned, we have used a detailed balance argument, whereby the unimolecular rate constant for back-dissociation is given by the equation

$$k_{\rm back} = k_{\rm capt}\frac{\rho(R)}{\rho(I)}, \quad (1)$$

where $k_{\rm capt}$ is the capture rate constant, $\rho(R)$ is the density of states per unit volume for the reactants and $\rho(I)$ is the density of states for the intermediate. For the intermediate dissociation into formamide + H, where, as opposed to the reactants, a well-defined transition state exists, we have performed an RRKM calculation. The microcanonical rate constant is calculated using the formula

$$k(E) = \frac{N(E)}{h\rho(E)}, \quad (2)$$

where $N(E)$ denotes the sum of states in the transition state at energy E, $\rho(E)$ is the reactant density of states at energy E and h is Planck's constant. $N(E)$ is obtained by integrating the relevant density of states up to energy E and the rigid rotor/harmonic oscillator model is assumed. Both densities of states (reactant and transition state) are appropriately symmetrized with respect to the number of identical configurations of the reactants and/or transition state. Tunnelling and quantum reflection have been taken into account by computing the tunnelling probability for an Eckart barrier having the same negative second derivative at the maximum of the pertinent saddle point. After all calculations have been performed, the branching ratio between products and back-dissociation is determined for each energy and the corresponding capture rate constant is multiplied by this ratio to give the rate constant for the formation of formamide. Finally, the rate constants are Boltzmann-averaged in order to provide the rate constants as a function of temperature.

3 RESULTS

3.1 Electronic and vibrational investigations

The structures of all the molecules were optimized at the B2PLYP-D3/m-aug-cc-pVTZ and CBS-QB3 levels of theory. All the precursors, intermediate and products were fully characterized as minima on the PES and transition states exhibited a single imaginary frequency thanks to vibrational calculations at B2PLYP-D3/m-aug-cc-pVTZ level.

Fig. 1 depicts the possible path of the full $CH_2O + NH_2 \rightarrow NH_2CHO + H$ formation reaction and the relative electronic energies of all the involved compounds, obtained at the CBS-QB3 level. Zero-point energies (ZPE) issuing from B2PLYP-D3BJ/m-aug-cc-pVTZ harmonic frequencies were added to CBS-QB3 electronic energies to obtain the 0 K free energies (of course identical to enthalpies) also shown in Fig. 1. The proposed pathway includes one intermediate (1) and one transition state (2). In the first step of the reaction the NH_2 radical attacks the carbon atom of formaldehyde, leading to the $H_2C(NH_2)O$ radical 1, that is about 71 kJ mol^{-1} more stable than the precursors. This step is followed by hydrogen loss from the carbon atom, leading to formamide together with H radical, and ruled by the transition state 2, which exhibits a 67 kJ mol^{-1} barrier (reduced to 46 kJ mol^{-1} if ZPE is included). The products were found to be ∼46 kJ mol^{-1} more stable than the reagents. The proposed radicalic mechanism is sketched in Fig. 2.

Alternative paths have been considered, including H migrations in compound 1 (from C and N to O atoms), NH_2 attack on the oxygen atom of formaldehyde or hydrogen abstraction from NH_2 which could have led to NH_3 and HCO. However, all these reaction channels are ruled by activation energies too high to be overcome in the interstellar medium (ISM). A plausible tautomeric form of formamide was also investigated, but once again the corresponding reaction channel is closed under the typical conditions of the ISM.

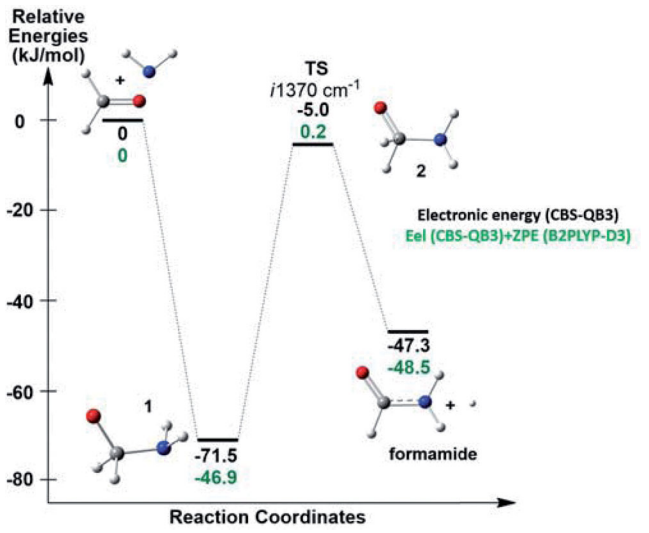

Figure 1. Proposed reaction path for formamide formation. The *y*-axis reports the relative electronic energies (black: CBS-QB3) and zero-point corrected energies at 0 K (green: B2PLYP-D3/m-aug-cc-pVTZ harmonic frequencies).

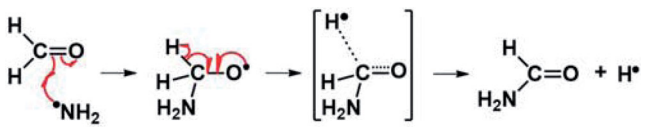

Figure 2. Possible radical mechanism for formamide formation.

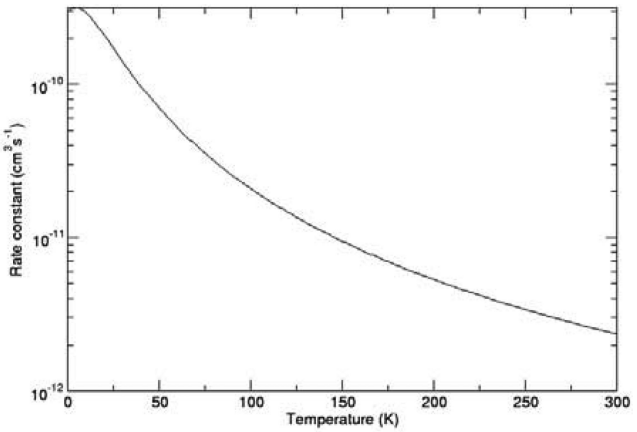

Figure 3. Total bimolecular rate constant for formamide formation as a function of temperature.

3.2 Kinetics

Fig. 3 shows the variation of the computed rate constant for formamide formation as a function of temperature up to 300 K. The calculated rate constants have also been fitted, for temperatures from 10 K onwards, to an expression of the form:

$$k(T) = A \times (T/300)^{\beta} e^{-\gamma/T} \quad (3)$$

with $A = 2.6 \times 10^{-12}$ cm^3 s^{-1}, $\beta = -2.1$ and $\gamma = 26.9$ K. The rate constant decreases monotonically as the temperature increases.

Even though the activation energy governing H loss is marginally higher than the energy of the reactants, this difference is so small that, even at the lowest energies considered, tunnelling leads to an appreciable rate for hydrogen loss. In fact, at low energies (and temperatures), H loss largely predominates over back-dissociation. The rates of the two processes become equal around 10 K and then, as the energy increases further, the rate of back-dissociation increases much faster than the one for H loss due to the more rapid increase of the density of states of the reactants (which include free rotations) and, as a result, the rate for formamide formation drops.

Fig. 4 shows the unimolecular rate constant and back-dissociation as a function of energy.

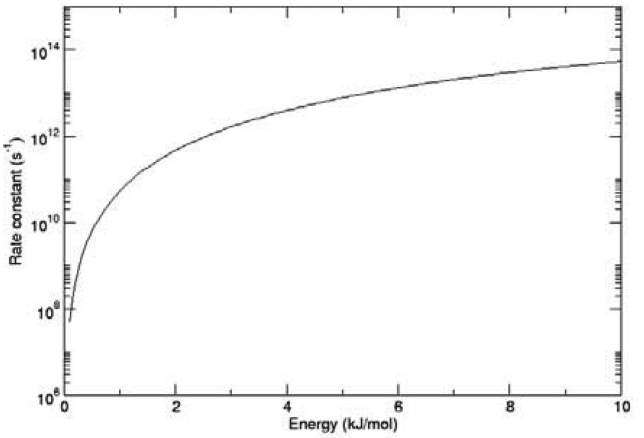

Figure 4. Unimolecular rate constant for dissociation to reactants of initial intermediate as a function of total energy.

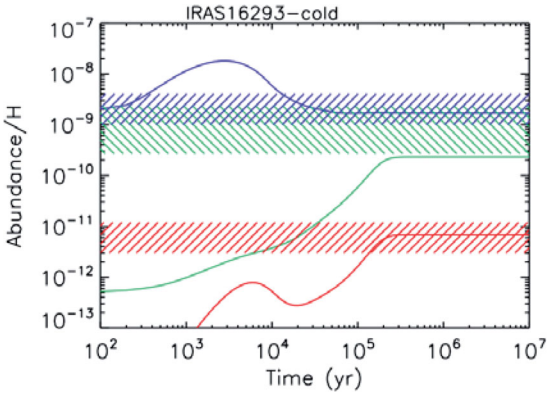

Figure 5. Abundances (with respect of H atoms) in the cold envelope of IRAS16293-2422 as a function of time (in years): H_2CO (blue), NH_2CHO (red) and NH_2 (green). The dashed boxes show the relevant measured values.

3.3 Astrochemical modelling

In order to test the impact of the new rates on the predictions of the formamide abundance, we run a series of models with the aim to reproduce the observations in two different objects: the cold envelope of the Sun-like protostar IRAS16293-2422 (Jaber et al. 2014) and the molecular shock L1157-B2 (Mendoza et al. 2014). We chose these two cases because they represent two extreme conditions, with the lowest ($\sim 6 \times 10^{-12}$) and highest ($\sim 2 \times 10^{-8}$) measured abundance of formamide.[1] For the model, we used the time-dependent Nahoon code[2] (Wakelam et al. 2012). It resolves the gas-phase chemical equation as a function of the time, using the KIDA 2014 chemical network (Wakelam et al. 2015), containing 489 species and 7499 reactions. We corrected the rate coefficient of the $NH_2 + H_2CO$ reaction according the computations presented in the previous section. In the following, we will discuss the two cases of IRAS16293-2422 and L1157-B2 separately.

IRAS16293-2422, cold envelope: IRAS16293-2422 is a well-studied Sun-like protostar of 22 $L_\odot$ (e.g. Crimier et al. 2010; Caux et al. 2011). Specifically, the density of the envelope increases going inwards with a power law of $\sim$1.5, from an H_2 density of 2×10^5 cm^{-3} at 7000 au. The temperature also increases going inwards from 10 K at the border to 100 K at 85 au (Crimier et al. 2010). Kahane et al. (2013) detected the formamide using the unbiased spectral survey TIMASSS[3] (Caux et al. 2011). Successively, Jaber et al. (2014) modelled the formamide line emission to disentangle the contribution from the cold and the warm (hot corino) part of the IRAS16293-2422 envelope and found that the average formamide abundance in the cold envelope is $\sim 6 \times 10^{-12}$. For our chemical model, we used an average H density of 2×10^6 cm^{-3} and temperature of 20 K. We run the model assuming that the elemental abundances in Wakelam & Herbst (2008; table 1, column EA2) are depleted by a factor 10 (C, O and N) and 100 (the heavier elements), in agreement with previous observations. With these assumptions, the steady state abundance of NH_2CHO, H_2CO and NH_2 result in excellent agreement with the observed values, as shown in Fig. 5. Note that the implicit assumption is that the cold envelope is formed by material previously present in the placental molecular cloud, whose age is $\geq 10^6$ yr.

[1] Note that the abundances here are given with respect to the H atoms, while in the original articles they are with respect to H_2.
[2] http://kida.obs.u-bordeaux1.fr.
[3] http://www-laog.obs.ujf-grenoble.fr/heberges/timasss/.

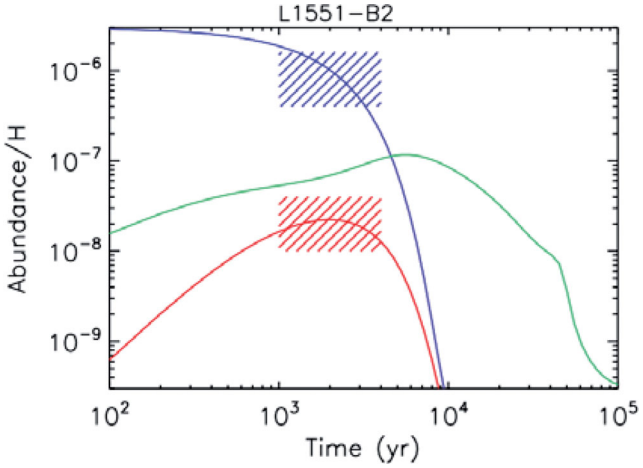

Figure 6. Abundances (with respect of H atoms) after the passage of the shock in L1157-B2 as a function of time (in years): H_2CO (blue), NH_2CHO (red) and NH_2 (green). The dashed boxes show the relevant measured values.

L1157-B2: L1157-B2 is a molecular shock which is part of the molecular outflow system emanating from L1157-mm (e.g. Gueth, Guilloteau & Bachiller 1996; Lefloch et al. 2012). This system has extensively been studied. Briefly, it is composed by two major ejection events, at the origin of two molecular shock sites: B2, created by the first event, and B1, created by the second one and which is spatially closer to the central object. B1 is the best studied of the two molecular shocks, as it has (also) been observed in the framework of two unbiased spectral surveys programs, CHESS (Ceccarelli et al. 2010; http://chess.obs.ujf-grenoble.fr/) and ASAI (Lefloch et al. in preparation; http://www.oan.es/ASAI), which provided the spectral coverage of the 500–2000 GHz with Herschel and the 3, 2 and 1 mm bands with IRAM-30 m, respectively. Mendoza et al. (2014) measured the formamide abundance in B2 and B1, equal to $\sim 2 \times 10^{-8}$ and $\sim 1 \times 10^{-8}$, respectively. Relevant to the simulations reported here, Lefloch et al. (2012) provided constrains on the B1 density and temperature, $\sim$70 K and $\sim 10^5$ cm^{-3}, respectively. Podio et al. (2014) used the line emission from several molecular ions to further constrain the cosmic ray ionization rate in the region, 3×10^{-16} s^{-1}, a parameter important in chemistry as it influences the time-scale of the chemical evolution. We adopted the above values also for the B2 molecular shock. The model, as in previous works (Mendoza et al. 2014; Podio et al. 2014), consists in a two-step procedure: (1) in the first step, the steady chemical abundances are computed assuming that the elemental abundances in Wakelam et al. (2008, table 1, column EA2) are depleted by a factor 10 (C, O and N) and 100 (the heavier elements); (2) in the second step, CO, H_2O, H_2CO and NH_3[4] are injected in the gas phase, to simulate the passage of the shock, and the chemical evolution is followed until a few 10^4 yr, even though the age of the B1 shock is evaluated to be around 2000 yr and the B2 a bit older. The CO and the H_2O abundances (with respect to H) are 8×10^{-5} and 1×10^{-4}, respectively. We run several models varying the H_2CO and NH_3 abundances. Fig. 6 shows the abundance of NH_2CHO, H_2CO and NH_2 obtained assuming H_2CO and NH_3 abundances equal to 3×10^{-6} and 1×10^{-6}, respectively, in agreement with their measurements by Mendoza et al. (2014) and Tafalla & Bachiller (1995). The dashed areas

[4] NH_2 is then synthesized by NH_3, which is the N-element iced major reservoir (e.g. Boogert et al. 2015).

show the measured values of NH_2CHO and H_2CO.[5] The predictions obtained using the new values perfectly reproduce the observations between 1000 and 3000 yr, the estimated age of the shock. The predicted NH_2 abundance is about 5–9 $\times$ 10^{-8}.

We also run a few models for the specific case describing B1. We can reproduce the measured formamide abundance and predict an NH_2 abundance of $\sim 10^{-8}$. From the Mendoza et al. (2014) upper limit, we derive a 3σ level upper limit on the NH_2 abundance of $\sim 3 \times 10^{-9}$, which is a factor $\sim$3 lower than the predicted one. We caution that these upper limits suffer of the uncertainty on the excitation temperature, and, therefore, further dedicated observations should be carried out to better constraint the predictions.

In summary, the new rate for the reaction H_2CO and $NH_2 \rightarrow NH_2CHO + H$ allows gas phase reactions fully justify the observed formaldehyde abundances, both in the cold and warm gas sources, without the need to invoke specific grain-surface reactions for that.

4 CONCLUSION AND PERSPECTIVES

In this paper, we have provided new insights concerning the formation of formamide in the ISM. Our computations allowed us to propose a reaction path combined to a plausible mechanism concerning this formation. Indeed, the first addition step does not involve any barrier and can therefore occur in space. RRKM calculations confirmed the feasibility of this reaction since once this first addition is done, formamide formation largely predominates over back-dissociation at low energies. Moreover, we tested the impact of these new kinetic data on the prediction of formamide abundance, comparing it with observations in the cold envelope of the Sun-like protostar IRAS16293-2422 and the molecular shock L1157-B2 (lowest and highest measured abundance of formamide). The results obtained from these simulations are in excellent agreement with the observation and, therefore, confirmed our computational protocol.

A more general conclusion is that neutral–neutral gas-phase reactions can account for the formation of relatively complex organic molecules even under the extreme conditions of ISM. Grain-surface reactions are often called into play to explain the formation of complex organic molecules because of supposedly missing formation routes in the gas phase. However, not all the possible gas-phase routes have been actually explored, either in laboratory experiments or theoretically, or correctly included in the astrochemical networks and models (see, for instance, Balucani, Ceccarelli & Taquet 2015). Other studies of critical and yet unexplored neutral–neutral gas phase reactions performed with the same theoretical methods employed here can help to fulfil the gap of the missing reactions leading to complex organic molecules, especially when those reactions cannot be easily investigated in laboratory experiments.

ACKNOWLEDGEMENTS

We wish to thank J-C. Loison for fruitful discussions. We acknowledge the financial support from the COST Action CM1401 'Our Astrochemical History'. NB acknowledges the financial support from the Université Grenoble Alpes and the Observatoire de Grenoble. The research leading to these results has received funding from the European Research Council under the European Union's Seventh Framework Programme (FP/2007-2013)/ERC grant agreement no. [320951].

[5] The upper limit on the NH_2 in Mendoza et al. (2014) strictly applies to B1, where the NH_2 were observed but not detected. In the case of B2, there are no specific observations.

REFERENCES

Adande G. R., Woolf N. J. G., Ziurys L. M., 2011, Astrobiology, 13, 439
Balucani N., Ceccarelli C., Taquet V., 2015, MNRAS, 449, L16
Bisschop S. E., Jørgensen J. K., van Dishoeck E. F., de Wachter E. B. M., 2007, A&A, 465, 913
Biver N. et al., 2014, A&A, 566, L5
Bockelee-Morvan D. et al., 2000, A&A, 53, 1101
Boogert A. C. A., Gerakines P. A., Whittet D. C. B., 2015, Annu. Rev. Astron. Astrophys., 53, in press
Caselli P., Ceccarelli C., 2012, A&AR, 20, 56
Caux E. et al., 2011, A&A, 532, A23
Ceccarelli C. et al., 2010, A&A, 521, L22
Crimier N., Ceccarelli C., Maret S., Bottinelli S., Caux E., Kahane C., Lis D. C., Olofsson J., 2010, A&A, 519, 65
Dunning T. H., 1989, J. Chem. Phys., 90, 1007
Frisch M. J. et al., 2013, Gaussian09 GDVH32. Gaussian, Inc., Wallingford CT
Garrod R. T., 2013, ApJ, 765, 60
Garrod R. T., Weaver S. L. W., Herbst E., 2008, ApJ, 682, 283
Goerigk L., Grimme S., 2011, J. Chem. Theory Comput., 7, 291
Grimme S. J., 2006, Chem. Phys., 124, 034108
Grimme S., Ehrlich S., Goerigk L., 2011, J. Comput. Chem., 32, 1456
Gueth F., Guilloteau S., Bachiller R., 1996, A&A, 307, 891
Halfen D. I., Ilyushin V., Ziurys L. M., 2011, ApJ, 743, 60
Hollis J. M., Lovas F. J., Remijan A. J., Jewell P. R., Ilyushin V. V., Kleiner I., 2006, ApJ, 643, L25
Jaber A. A., Ceccarelli C., Kahane C., Caux E., 2014, ApJ, 791, 29
Jones B. M., Bennett C. J., Kaiser R. I., 2011, ApJ, 734, 78
Kahane C., Ceccarelli C., Faure A., Caux E., 2013, ApJ, 763, L38
Lefloch B. et al., 2012, ApJ, 757, L25
Leonori F. et al., 2009, J. Phys. Chem. A, 113, 15328
Leonori F., Skouteris D., Petrucci R., Casavecchia P., Rosi M., Balucani N., 2013, J. Chem. Phys., 138, 024311
Li Q. S., Lu R. H., 2002, J. Phys. Chem. A, 106, 9446
Lopez-Sepulcre A. et al., 2015, MNRAS, 449, 2438
Mendoza E., Lefloch B., López-Sepulcre A., Ceccarelli C., Codella C., Boechat-Roberty H. M., Bachiller R., 2014, MNRAS, 445, 151
Montgomery J. A., Frisch M. J., Ochterski J. W., Petersson G. A., 2000, J. Chem. Phys., 112, 6532
Noble J. A. et al., 2015, A&A, 576, 91
Ochterski J. W., Petersson G. A., Montgomery J. A., 1996, J. Chem. Phys., 104, 2598
Papajak E. et al., 2009, J. Chem. Theory Comput., 5, 1197
Podio L., Lefloch B., Ceccarelli C., Codella C., Bachiller R., 2014, A&A, 565, 64
Quan D., Herbst E., 2007, A&A, 474, 521
Redondo P., Barrientos C., Largo A., 2014a, ApJ, 780, 181
Redondo P., Barrientos C., Largo A., 2014b, ApJ, 793, 32
Rubin R. H., Swenson G. W., Jr, Benson R. C., Tigelaar H. L., Flygare W. H., 1971, ApJ, 169, L39
Saladino R., Botta G., Pino S., Costanzo G., Di Mauro E., 2012, Chem. Soc. Rev. 41, 5526
Tafalla M., Bachiller R., 1995, ApJ, 443, L37
Turner B. E., 1989, ApJS, 70, 539
Vazart F. et al., 2015, ApJ, in press
Vazart F., Latouche C., Skouteris D., Balucani N., Barone V., 2015, ApJ, in press
Wakelam V., Herbst E., 2008, ApJ, 680, 371
Wakelam V. et al., 2012, ApJS 199, 21
Wakelam V. et al., 2015, ApJS 217, 20
Walsh C., Millar T. J., Nomura H., Herbst E., Widicus Weaver S., Aikawa Y., Laas J. C., Vasyunin A. I., 2014, A&A 563, 33
Yamaguchi T. et al., 2012, PASJ, 64, 105

This paper has been typeset from a TEX/LATEX file prepared by the author.